Variations in the Earth's Orbit: Pacemaker of the Ice Ages

Article *in* Science · January 1977

DOI: 10.1126/science.194.4270.1121 · Source: PubMed

J. D. Hays
Lamont - Doherty Earth Observatory Columbia University

Reprinted from
10 December 1976, Volume 194, pp. 1121-1132

SCIENCE

Variations in the Earth's Orbit: Pacemaker of the Ice Ages

J. D. Hays, John Imbrie, N. J. Shackleton

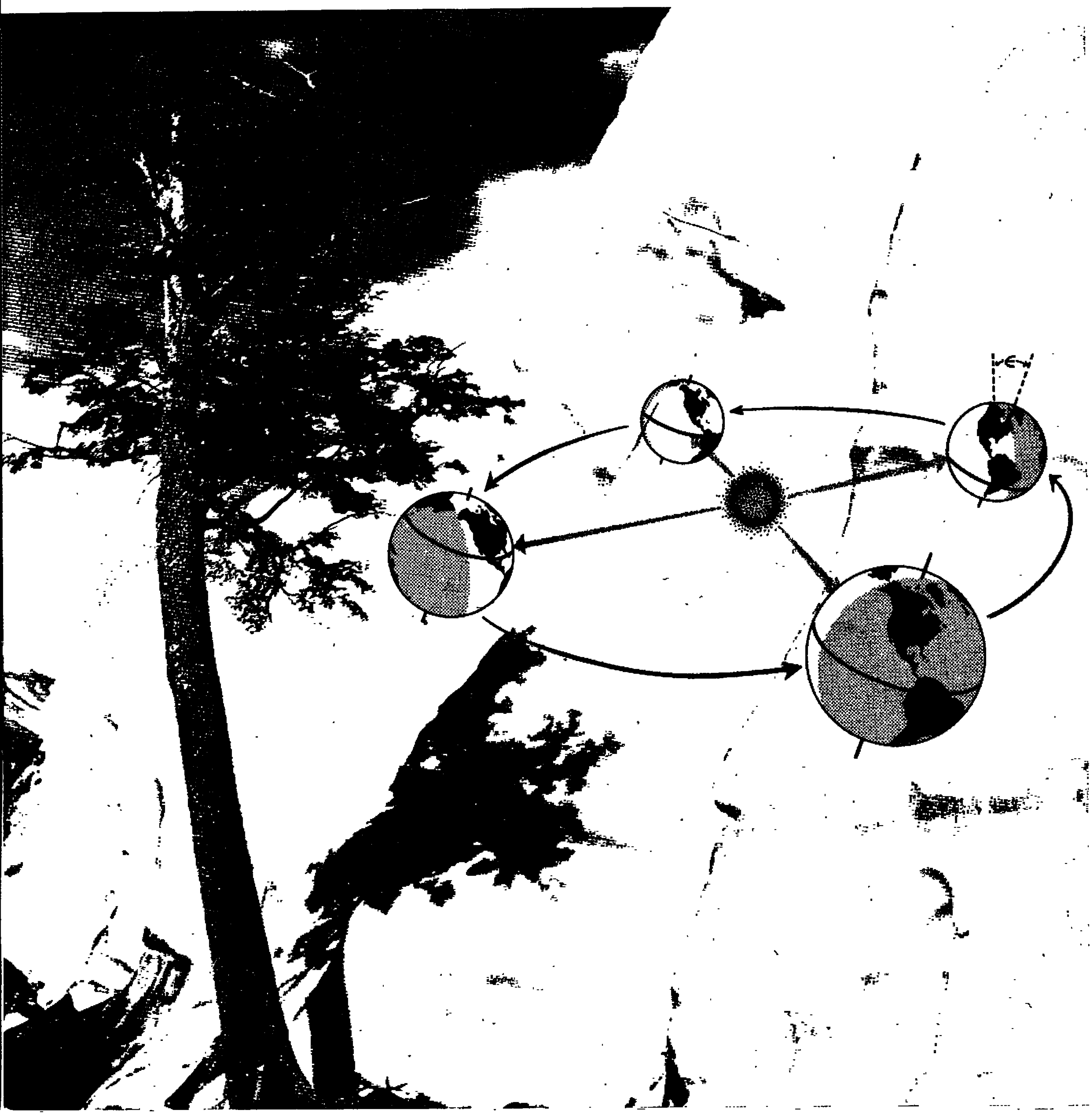

COVER

Moreno Glacier at Lago Argentino in the Andes of Argentina with its terminus advancing into a stand of southern beech (*Nothofagus pumilio*) [J. H. Mercer, Ohio State University, Columbus]. The orbital diagram [G. Kukla, Lamont-Doherty Geological Observatory, Palisades, New York] symbolizes conclusion of research that variations in the earth's orbit are the fundamental cause of the succession of late Pleistocene ice ages. See page 1121.

10 December 1976, Volume 194, Number 4270 **SCIENCE**

Variations in the Earth's Orbit: Pacemaker of the Ice Ages

For 500,000 years, major climatic changes have followed variations in obliquity and precession.

J. D. Hays, John Imbrie, N. J. Shackleton

For more than a century the cause of fluctuations in the Pleistocene ice sheets has remained an intriguing and unsolved scientific mystery. Interest in this problem has generated a number of possible explanations (*1*, *2*). One group of theories invokes factors external to the climate system, including variations in the output of the sun, or the amount of solar energy reaching the earth caused by changing concentrations of interstellar dust (*3*); the seasonal and latitudinal distribution of incoming radiation caused by changes in the earth's orbital geometry (*4*); the volcanic dust content of the atmosphere (*5*); and the earth's magnetic field (*6*). Other theories are based on internal elements of the system believed to have response times sufficiently long to yield fluctuations in the range 10^4 to 10^6 years. Such features include the growth and decay of ice sheets (*7*), the surging of the Antarctic ice sheet (*8*); the ice cover of the Arctic Ocean (*9*); the distribution of carbon dioxide between atmosphere and ocean (*10*); and the deep circulation of the ocean (*11*). Additionally, it has been argued that as an almost intransitive system, climate could alternate between different states on an appropriate time scale without the intervention of any external stimulus or internal time constant (*12*).

Among these ideas, only the orbital hypothesis has been formulated so as to predict the frequencies of major Pleistocene glacial fluctuations. Thus it is the only explanation that can be tested geologically by determining what these frequencies are. Our main purpose here is to make such a test.

Previous work has provided strong suggestive evidence that orbital changes induced climatic change (*13*–*20*). However, two primary obstacles have led to continuing controversy. The first is the uncertainty in identifying which aspects of the radiation budget are critical to climatic change. Depending on the latitude and season considered most significant, grossly different climatic records can be predicted from the same astronomical data. Milankovitch (*4*) followed Koppen and Wegener's (*21*) view that the distribution of summer insolation (solar radiation received at the top of the atmosphere) at 65°N should be critical to the growth and decay of ice sheets. Hence the curve of summer insolation at this latitude has been taken by many as a prediction of the world climate curve. Kukla (*19*) has pointed out weaknesses in Koppen and Wegener's proposal and has suggested that the critical time may be September and October in both hemispheres. However, several other curves have been supported by plausible arguments. As a result, dates estimated for the last interglacial on the basis of these curves have ranged from 80,000 to 180,000 years ago (*22*).

The second and more critical problem in testing the orbital theory has been the uncertainty of geological chronology. Until recently the inaccuracy of dating methods limited the interval over which a meaningful test could be made to the last 150,000 years. Hence the most convincing arguments advanced in support of the orbital theory to date have been based on the ages of 80,000, 105,000, and 125,000 years obtained for coral terraces first on Barbados (*15*) and later on New Guinea (*23*) and Hawaii (*24*). These structures record episodes of high sea level (and therefore low ice volume) at times predicted by the Milankovitch theory. Unfortunately, dates for older terraces are too uncertain to yield a definitive test (*25*).

More climatic information is provided by the continuous records from deep-sea cores, especially the oxygen isotope record obtained by Emiliani (*26*). However, the quasi-periodic nature of both the isotopic and insolation curves, and the uncertain chronology of the older geologic records, have combined to render plausible different astronomical interpretations of the same geologic data (*13*, *14*, *17*, *27*).

Strategy

All versions of the orbital hypothesis of climatic change predict that the obliquity of the earth's axis (with a period of about 41,000 years) and the precession of the equinoxes (period of about 21,000 years) are the underlying, controlling variables that influence climate through their impact on planetary insolation. Most of these hypotheses single out

The authors are all members of the CLIMAP project. J. D. Hays is professor of geology at Columbia University, New York 10027, and is on the staff of the Lamont-Doherty Geological Observatory, Palisades, New York 10964. John Imbrie is Henry L. Doherty professor of oceanography, Brown University, Providence, Rhode Island 02912. N. J. Shackleton is on the staff of the Sub-department of Quaternary Research, Cambridge University, Cambridge, England.

mechanisms of climatic change which are presumed to respond to particular elements in the insolation regime (*28*). In our more generalized version of the hypothesis we treat secular changes in the orbit as a forcing function of a system whose output is the geological record of climate—without identifying or evaluating the mechanisms through which climate is modified by changes in the global pattern of incoming radiation (*29*). Most of our climatic analysis is based on the simplifying assumption that the climate system responds linearly to orbital forcing. The consequences of a more realistic, nonlinear response are examined in a final section here.

Our geological data comprise measurements of three climatically sensitive parameters in two deep-sea sediment cores. These cores were taken from an area where previous work shows that sediment is accumulating fast enough to preserve information at the frequencies of interest. Measurements of one variable, the per mil enrichment of oxygen-18 ($\delta^{18}O$), make it possible to correlate these records with others throughout the world, and to establish that the sediment studied accumulated without significant hiatuses and at rates which show no major fluctuations.

To be used in tests of the orbital hypothesis, these data are transformed into geological time series. In our first test we make the simplest geochronological assumption, that sediment accumulated in each core at a constant rate throughout the period of study. Later we relax this assumption and allow slight changes in accumulation rate, as indicated by additional geochronological data.

Our frequency-domain tests use the numerical techniques of spectral analysis and are designed to seek evidence for a concentration of spectral energy at the frequencies of variation in obliquity and precession. We consider that support for the hypothesis can be decisive if both frequencies are detected and, to allow for geochronological uncertainties, if it can be clearly demonstrated that the ratio of the two frequencies detected does not differ significantly from the predicted ratio (about 1.8).

Finally, our time-domain tests are designed to examine the phase coherence between the three climatic records and between each record and the postulated forcing function. To this end we use the numerical techniques of bandpass filter analysis. Such an approach makes it possible to examine separately the variance components of the geological records that correspond in frequency to the variations of obliquity and precession.

Methods

Core selection. From several hundred cores studied stratigraphically by the CLIMAP project, we selected two (RC11-120 and E49-18) whose locations (Fig. 1 and Table 1) and properties make them ideal for testing the orbital hypothesis. Most important, they contain together a climatic record that is continuous, long enough to be statistically useful (450,000 years), and characterized by accumulation rates fast enough (> 3 centimeters per 1,000 years) to resolve climatic fluctuations with periods well below 20,000 years. In addition, the cores are centrally located between Africa, Australia, and Antarctica, and therefore little influenced by variations of erosional detritus from these continents. Finally, as explained below, a Southern Hemisphere location provides an opportunity to monitor simultaneously both Northern Hemisphere ice volume and Southern Hemisphere temperature. No other cores known to us have all these attributes.

Geological data. We have measured (i) $\delta^{18}O$, the oxygen isotopic composition of planktonic foraminifera; (ii) *Ts*, an estimate of summer sea-surface temperatures at the core site, derived from a statistical analysis of radiolarian assemblages; and (iii) percentage of *Cycladophora davisiana*, the relative abundance of a radiolarian species not used in the estimation of *Ts*. Identical samples were analyzed for the three variables at 10-cm intervals through each core (*30*).

Oxygen isotope analyses have been made in tests of *Globigerina bulloides* by well-established techniques (*31, 32*). The

Table 1. Core locations and depths.

Core	Length (cm)	Water depth (m)	Latitude	Longitude
RC11-120	954	3135	43°31′S	79°52′E
E49-18	1459	3256	46°03′S	90°09′E

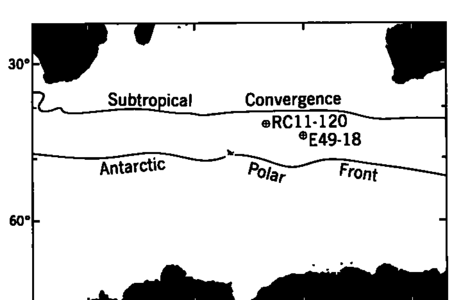

Fig. 1. Locations of cores in the southern Indian Ocean.

reproducibility for independent sampl
from the sediment is about ± 0.1 per m
[1 standard deviation (S.D.)]. Tests of *C
bulloides* are formed primarily at som
depth below the sea surface so th
changes in surface temperature do n
greatly affect the temperature at whic
the carbonate is secreted. Down-co
variations in $\delta^{18}O$ reflect changes in oc
anic isotopic composition, caused p
marily by the waxing and waning
Northern Hemisphere ice sheets (*31, 3*
Thus, the $\delta^{18}O$ in our subantarctic cor
is a Northern Hemisphere climatic re
ord.

Estimates of *Ts* were made by appl
ing statistical techniques (*18*) to suba
arctic radiolarians. The data base f
writing the transfer functions has be
expanded from that of Lozano and Ha
(*34*) by G. Irving and J. Morley to
clude cores in the vicinity of E49-18. T
accuracy of *Ts* as an estimate of s
surface temperature is ± 1.5°C; its rep
ducibility as an index of faunal change
± 0.32°C (1 S.D.).

The percentage of *C. davisiana* re
tive to all other radiolarians was det
mined by techniques previously
scribed (*35*). These counts have a p
cision of about ± 0.74 percent (1 S.D
The recent distribution of the cosmop
tan species *C. davisiana* Petrushevsk
shows no relation to present sea-surf
temperature (*34, 36*), so that the rema
able Pleistocene abundance variation
this species (which comprised up to
percent of the fauna during glacial m
ma in some areas) are also probably
due to temperature (*35*). The unique h
abundance of this species in recent s
ments of the Sea of Okhotsk has b
related to the structure of summer
face waters, where a low-salinity surf
layer is underlain by a strong tem
ature minimum (*37*). The high abunda
of *C. davisiana* during glacial time
the Antarctic may be due to a sim
surface water structure.

Measurements of these parame
therefore reflect changes in three part
the climate system: Northern He
sphere land ice, subantarctic sea-surf
temperature, and Antarctic surface
ter structure.

Orbital data. Since the pionee
work of Milankovitch (*4*) the chron
gies for orbital and insolation cha
have been recalculated several ti
(*38–40*). These papers and those of K
la (*19*) should be consulted for an ex
nation and evaluation of the nume
procedures used and for a discussio
the manner in which orbital changes
on the earth's insolation regime
function of latitude, season, and t

en Vernekar's (39) calculations are ıpared with those of Berger (40), the ing of inflection points in the obliquity precession curves do not differ by :e than 1000 years over the past ,000 years. For intervals older than ,000 years ago, however, discrepan- ; between the calculations become ıificant, and the work of Berger is to preferred because it includes the ef- t of higher-order terms.

›logical Time Series

'tratigraphic sequence. Because the Ↄ record in deep-sea sediments pri- rily reflects global ice volume, it is bally synchronous in open-ocean 'es and provides (along with standard ›stratigraphical techniques) a basic ıtigraphy for the last million years (33, 42). This stratigraphy has a resolu- n limited only by ocean mixing (about)0 years) and bioturbation. The $\delta^{18}O$:ord was divided by Emiliani (26) into mbered stratigraphic stages, which are ɜd here.

The oxygen isotope record in core :11-120 is complete and typical back to e stage 9 (Fig. 2). Stage 5 shows its aracteristic three peaks (26, 42); and ıge 7 is interrupted by a sharp positive cursion, which is typical (31, 42).

In core E49-18 (Fig. 3) the high per- ntage of *C. davisiana* at the top in- :ates that the Holocene is missing (35); ɜ top may be as old as 60,000 years. In dition, visual inspection of the core ows that it has been mechanically :etched between 300 and 400 cm during e coring process. Consequently, the ıre was analyzed for $\delta^{18}O$ only from the wer part of stage 5 to the base. The cord of stages 6 to 9 is similar to the ıuivalent part of core RC11-120; the mainder can be compared stage by age with other cores (31, 42). As in .her cores studied, stage 12 is bracketed ı the extinction of the coccolith *Pseu- ›emiliania lacunosa* below (43) and the ıdiolarian *Stylatractus universus* above '4). This confirms the presence of the ıtire oxygen isotope sequence from .age 6 to stage 13.

The *Ts* curve in both cores differs ıarkedly in shape from the $\delta^{18}O$ curve, eing characterized by abrupt increases f estimated temperature of up to 6°C in tage 1 and at the base of stages 5, 7, 9, nd 11. Elsewhere in the cores *Ts* fluctua- .ons do not exceed 3°C. The spiky char- cter of this record is similar to that of ertain Atlantic cores from high northern ıtitudes (45).

Above stage 10 there is near synchro- neity between the $\delta^{18}O$ minima and *Ts* maxima. However, changes in *Ts* pre- cede changes in $\delta^{18}O$ by a small amount; this is most evident at extreme *Ts* maxi- ma. We conclude that over this time interval changes in Northern Hemi- sphere ice volume and subantarctic sea- surface temperature are nearly synchro- nous. Between stage 10 and the upper part of stage 11, however, the higher- frequency fluctuations in *Ts* and $\delta^{18}O$ appear to be out of phase; and the low- temperature extremes are colder than they are at higher levels in the cores.

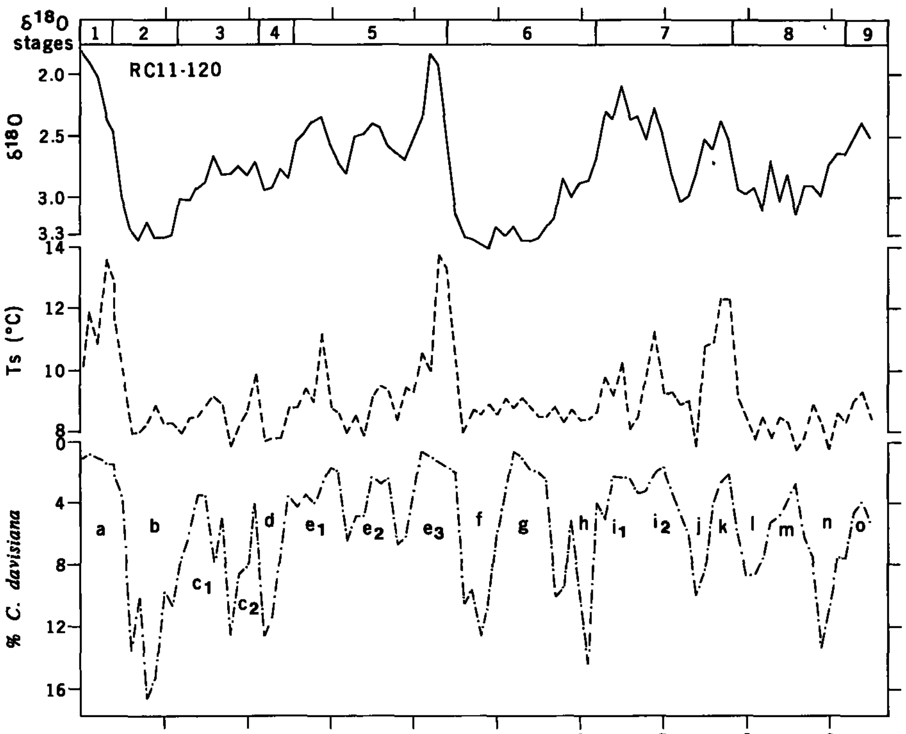

Fig. 2. Depth plots of three parameters measured in core RC11-120: $\delta^{18}O$ (solid line), *Ts* (dashed line), and percentage of *C. davisiana* (dash-dot line). Letter designations of peaks on the latter curve are informal designations of various parts of the record.

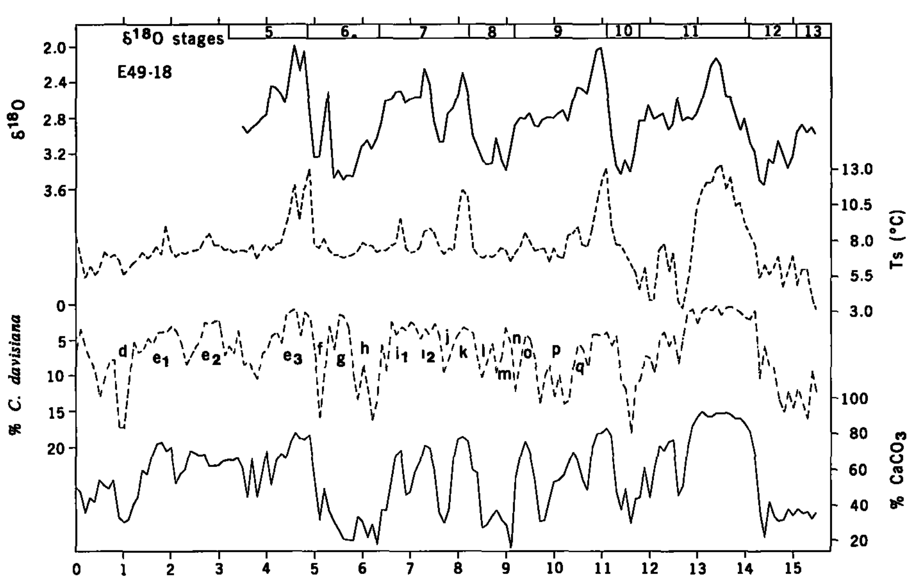

Fig. 3. Depth plots of four parameters measured in core E49-18: $\delta^{18}O$ (solid line at the top), *Ts* (dashed line), percentage of *C. davisiana* (dash-dot line), and percentage of $CaCO_3$ (solid line at the bottom). The technique used for $CaCO_3$ measurement is that of Hülsemann (81). A comparison of the lettered intervals of the *C. davisiana* curve for this core with those for core RC11-120 (Fig. 2) shows that the time represented by the top 1.5 m of RC11-120 is not present in E49-18.

Table 2. Chronologic assumptions of age models. Interpolation within and extrapolation beyond control points shown is linear. For the combined PATCH ELBOW and PATCH TUNE-UP records, data from 0 to 785 cm in RC11-120 were combined with data below 825 cm in E49-18.

Age model	Core	Depth (cm)	Age (× 10^3 years)	Sedimentation rate (cm/10^3 years)
SIMPLEX	RC11-120	0	0	3.46
		440	127*	
	E49-18	490	127*	2.92
		1405	440†	
ELBOW	RC11-120	0	0	
		39	9.4‡	4.14
		440	127*	3.40
		785	251†	2.78
	E49-18	490	127*	
		825	251†	2.70
		1405	440†	3.06
TUNE-UP	RC11-120	0	0	
		39	9.4‡	4.14
		440	127*	3.40
		785	247	2.87
	E49-18	490	127*	
		825	247	2.79
		1405	425	3.26

*Age of isotopic stage 6–5 boundary (17). †Age of isotopic stage 8–7 boundary (251,000 years) and boundary 12–11 (440,000 years) (31). ‡Carbon-14 determination (35).

Table 3. Frequency-domain test of orbital theory based on SIMPLEX chronology for two deep-sea cores. Values are mean periods (in thousand years per cycle) of peaks in unprewhitened geologic and orbital spectra.

Geologic data						Orbital data	
Core	Time interval (× 10^3 B.P.)	Frequency band	*Ts*	$\delta^{18}O$	*C. davisiana* (%)	Spectral estimate	Element
		a	87	91	106		
RC11-120	0–273*	*b*	38	38	37	40.8	Obliquity (ϵ)
		c	21	23		22.6	Precession (*P*)
		b/c	1.8	1.7		1.8	ϵ/P
		a	94	109	119		
E49-18	127–489†	*b*	43	47		41.1	Obliquity (ϵ)
		c	24	24		21.9	Precession (*P*)
		b/c	1.8	1.9		1.9	ϵ/P

*Geologic and orbital spectra for this interval were calculated with $n = 91$ and $m = 40$ (57). †Geologic and orbital spectra for this interval were calculated with $n = 121$ and $m = 50$ (57).

Table 4. Frequency-domain test of orbital theory using ELBOW chronology for PATCH core. Values are mean periods (in thousand years per cycle) of peaks and subpeaks in geologic and orbital spectra [$n = 163$ and $m = 50$ (57)]. Orbital data calculations cover the past 468,000 years.

	Geologic data						Orbital data		
	Unprewhitened spectra			Prewhitened spectra					
Frequency band	*Ts*	$\delta^{18}O$	*C. davisiana* (%)	*Ts*	$\delta^{18}O$	*C. davisiana* (%)	Spectral estimate	Time domain estimate	Element
a	94	106	122				105	97	Eccentricity (*e*)
b	40	43	43	42	43*	42*	41.1	40.6	Obliquity (ϵ)
c_1	23	24	24	24*	24	24	23.1		Precession (P_1)
c_m				22*	22	22	21.8	21.6	Precession (P_m)
c_2		19.5		19.5	19.5	19.5	18.8		Precession (P_2)
b/c_1	1.7	1.8	1.8	1.8	1.8	1.7	1.78		ϵ/P_1

*Peaks in prewhitened spectra are significant at $P = .05$.

Although the percentage *C. davisian* curve has a character distinct from th other two, its maxima are generally cor related in timing, but not in amplitude with *Ts* minima and $\delta^{18}O$ maxima, excep in stages 8 and 9.

Time control. A basic chronologic framework for these sequences is estab lished by determining the absolute age of certain horizons. In RC11-120, ca bon-14 dating at the 36- to 39-cm lev yields an age of 9400 ± 600 years (35 This level marks the most recent *Ts* max mum and substantially precedes th Northern Hemisphere hypsitherma which at many sites has been dated about 6000 years ago (1).

The age of the boundary betwee stage 12 and stage 11 was taken fro Shackleton and Opdyke (31), who es mated it at 440,000 years in an equatori Pacific core (V28-238) by assuming ur form accumulation between the core to and the magnetic reversal marking th Brunhes-Matuyama boundary. Extin tion of *S. universus* occurred globally this stage boundary (44), so that the es mates of 400,000 years for the age of th extinction (46) in the North Pacific a Antarctic constitute independent dete minations for the age of the 12-11 boun ary. The range of these figures express the current age uncertainty of this boun ary (47).

In many areas there is evidence fo change in accumulation rate arou stage 6 (48) so that we have used independent estimate of 251,000 ye for the stage 8-7 boundary. This es mate, like that for the 12-11 bounda was taken from Pacific core V28-238 (3

The age of the stage 6-5 boundary within the range of several radiomet dating techniques, and has been the c nerstone of some previous attempts support specific versions of the orbi hypothesis. We have used an age 127,000 years which has an analyti error estimated at ± 6000 years (17). this point in our analysis we do not exp iment with other published ages (49) cause it is very difficult to reconcile the terrace coral ages from Barbad New Guinea, and Hawaii (15, 23, 24, and data from deep-sea cores (51) w any substantially different age (52).

Chronological models. To test the bital theory, age models (Table 2) m be developed to express each geologi variable as a function of time. We do t by assuming that sediment accumula at a constant rate between the horiz for which we have independent e mates of age. Although uniform sedim tation is an ideal which is unlikely prevail precisely anywhere, the fact t characteristics of the oxygen isotope ord are present throughout the cores ;gests that there can be no substantial unae, while the striking resemblance records from distant areas shows that :re can be no gross distortions of accu- ılation rate.

SIMPLEX models assume uniform limentation rates through each core d fix the core top of RC11-120 at zero, : 6-5 stage boundary at 127,000 years ›res RC11-120 and E49-18), and the 12- stage boundary at 440,000 years (core 9-18; see Table 2). It is important to te that although the SIMPLEX model esents each variable as a function of e, the age estimated is an exact linear nction of depth in the core.

ELBOW models use more chronologi- l information and no longer represent e records as a simple function of depth 'able 2). Sedimentation rates change ghtly at three control points and are sumed constant between them.

PATCH is a time series in which we ıve joined the records of the two cores the 8-7 stage boundary, thereby pro- ding a longer and statistically more ;eful record. Another model in which ıe cores were joined at the 6-5 stage ɔundary was found to be statistically most identical and is not considered ere.

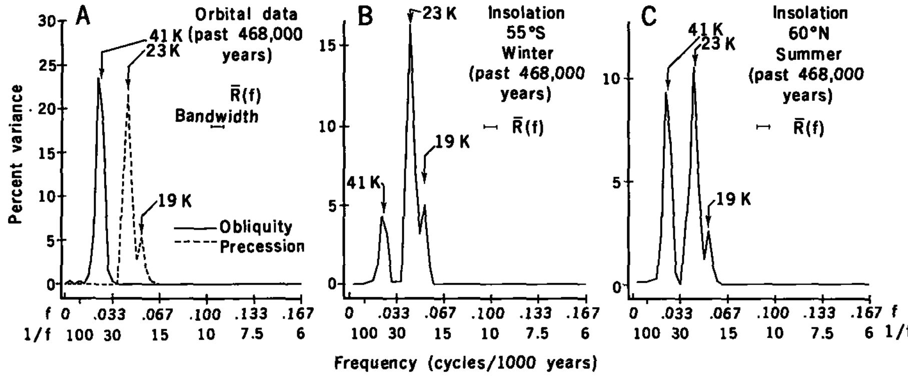

Fig. 4. High-resolution spectra of orbital and insolation variations over the past 468,000 years. Variance (as percentage of total variance per unit frequency band) is plotted as a function of frequency (cycles per thousand years). Arrows indicate weighted mean cycle lengths of spectral peaks (in thousands of years). (A) Spectra for obliquity and precession ($\Delta e \sin \Pi$). (B) Spectrum for winter insolation at 55°S. (C) Spectrum for summer insolation at 60°N. [All data are from Vernekar (*39*)]

requency-Domain Tests

Assumptions. From the viewpoint of near-systems modeling (*53*) the astro- omical theory of Milankovitch postu- ıtes two systems operating in series. 'he first is a radiation system which ransforms orbital signals (obliquity and ırecession) into a set of insolation sig- ıals (one for each combination of lati- ude and season). The insolation signals ıre transformed by a second, explicitly 'ormulated climate-response system into predicted) climate curves. In contrast, ve postulate a single, radiation-climate ;ystem which transforms orbital inputs nto climatic outputs. We can therefore ıvoid the obligation of identifying the ɔhysical mechanisms of climatic re- ;ponse and specify the behavior of the ;ystem only in general terms (*54*). The dynamics of our model are fixed by as- suming that the system is a time-in- variant, linear system—that is, that its behavior in the time domain can be de- scribed by a linear differential equation with constant coefficients. The response of such a system in the frequency do- main is well known: frequencies in the output match those of the input, but their amplitudes are modulated at different frequencies according to a gain function (*55*). Therefore, whatever frequencies characterize the orbital signals, we will expect to find them emphasized in pa- leoclimatic spectra (except for fre- quencies so high that they would be greatly attenuated by the time constants of response).

Numerical procedures. The statistical techniques we use to calculate both orbit- al and climatic spectra are taken without modification from the work of Blackman and Tukey (*56*) with elaborations by Jen- kins and Watts (*55*). Our procedure in- volves ten sequential steps: selection of an absolute chronology, calculation of a time series, detrending, prewhitening (optional), lagging, calculation of the autocovariance function, smoothing with a Hamming lag window, spectral estima- tion, scaling, and statistical evaluation (*57, 58*). In all calculations the sampling interval is fixed at 3000 years; hence the spectral estimates cover a frequency band ranging up to the Nyquist fre- quency of 0.167 cycle per thousand years.

Frequency analysis of astronomical data. For any particular latitude the in- tensity of solar radiation received at the top of the atmosphere varies quasi-peri- odically with three elements of the earth's orbit: eccentricity, obliquity, and the longitude of perihelion based on the moving equinox. Over the last 4 million years the eccentricity (e, the ratio of the focal distance to the length of the major axis) ranges from a value near zero to a maximum of about 0.06, and exhibits an average period of 93,000 years (*39*). Vari- ations in e, unlike variations in the other orbital elements, also slightly affect the total annual insolation received by the earth. Because the extreme range of this effect over the past 500,000 years is about 0.1 percent, it has generally been considered unimportant (*59*). Obliquity (ϵ, the angle between the equatorial and ecliptic planes) ranges from 22.1° to 24.5°, with an average period of about 41,000 years (*39*).

The climatic effect of precession is a function of Π, the longitude of perihelion based on the moving equinox, and e (*60*). Specifically, the intensity of incoming solar radiation at a particular latitude and season varies as $e \sin \Pi$. To express these variations as a time series, the value of $e \sin \Pi$ for June 1950 A.D. is subtracted from the same quantity calculated for particular times in the past. The resulting precessional index ($\Delta e \sin \Pi$) is approxi- mately equal to the deviation from its 1950 value of the earth-sun distance in June, expressed as a fraction of the semi- major axis of the earth's orbit (*61*). Over the past 4 million years, this index ranges from about +0.03 to −0.07 and has an average period of about 21,000 years (*39*).

We have used spectral techniques to analyze secular variations in ϵ, e, $\sin \Pi$, and $\Delta e \sin \Pi$ (*62*). Because these varia- tions are quasi-periodic, it is necessary to specify the interval over which fre- quencies are to be analyzed (*63*); our analyses (Tables 3 and 4 and Fig. 4) treat time intervals corresponding to the core records.

Spectra calculated for variations in ec- centricity and obliquity over the past 468,000 years (Table 4) are both uni- modal; that is, they have spectral peaks dominated by a single frequency (*64*). These spectral peaks correspond to cy- cles of 105,000 years (eccentricity) and 41,000 years (obliquity). Spectra calcu- lated for $\sin \Pi$ (not tabulated) and for $\Delta e \sin \Pi$ are more complex. Both are bi- modal, with subpeaks corresponding to cycles of 23,000 years (P_1) and 19,000 years (P_2).

We have also calculated spectra for two time series recording variations in insolation (Fig. 4), one for 55°S and the other for 60°N (*39*). To the nearest 1000 years, the three dominant cycles in these spectra (41,000, 23,000, and 19,000 years) correspond to those observed in the spectra for obliquity and precession. This result, although expected, underscores two important points. First, insolation spectra are characterized by frequencies reflecting obliquity and precession, but not eccentricity. Second, the relative importance of the insolation components due to obliquity and precession varies with latitude and season.

Frequency analysis of geological data. Using techniques identical to those applied to the astronomical data, we have calculated spectra for each of the three geological variables: *Ts*, $\delta^{18}O$, and percentage of *C. davisiana* (Fig. 5). The SIMPLEX chronology is used to analyze the individual cores, and the ELBOW chronology is applied to the combined (PATCH) core.

Because the SIMPLEX time series are undesirably short and are based on limited chronological control, we do not place much reliance on the accuracy of estimates of their constituent frequencies. Nevertheless, five of the six spectra calculated are characterized by three discrete peaks, which occupy the same parts of the frequency range in each spectrum (Table 3). Those corresponding to periods from 87,000 to 119,000 years are labeled *a*; 37,000 to 47,000 years *b*; and 21,000 to 24,000 years *c*. This suggests that the *b* and *c* peaks represent a response to obliquity and precession variation, respectively.

The ratios of obliquity period to precession period calculated for the intervals of time covered by cores RC11-120 and E49-18 are 1.8 and 1.9, respectively (Table 3). The observed ratios of the dominant period in peak *b* to the dominant period in peak *c* are 1.7 ± 0.1 and 1.9 ± 0.1 for RC11-120 and E49-18, respectively. Because the observed ratios from these geological data are independent of the ages used to calibrate the SIMPLEX time series and closely match ratios derived for orbital data, we conclude that the ratio test supports the hypothesis of orbital control.

To obtain accurate estimates of the climatic frequencies, we now examine spectra calculated from ELBOW time series for the combined (PATCH) tir series. As before, the climatic variance distributed mainly in three discrete spe tral peaks (Table 4 and Fig. 5). Mc than half of the total variance is cc tained in the low-frequency *a* peak (percent for *Ts*, 58 percent for $\delta^{18}O$, a 51 percent for *C. davisiana*). All thr peaks are unimodal. Estimates of t dominant cycle in the *a* peaks are 94,0(106,000, and 122,000 years for *Ts*, δ^{18} and percentage of *C. davisiana*, respe tively. Because these estimates are (rived from the low-frequency end of t spectrum, they should be regarded rough estimates. However, there can no doubt that a spectral peak center near a 100,000-year cycle is a major f(ture of the climatic record.

A substantial fraction of the variar is contained in the *b* peaks: 19 perc for *Ts*, 27 percent for $\delta^{18}O$, and 30 p cent for *C. davisiana* (Fig. 5). Each the three peaks is unimodal. Estimates this dominant cycle in the peaks rar from 40,000 to 43,000 years (Table 3)

A smaller fraction of the total variar is contained in the *c* peaks: 11 perc for *Ts*, 9 percent for $\delta^{18}O$, and 7 perc for *C. davisiana*. The *Ts* and *C. davis na* peaks, both unimodal, correspond cycles of 23,000 and 24,000 years, resp tively (Table 4). The *c* peak in the δ spectrum is bimodal, with subpeaks and c_2) corresponding to cycles of 24, and 19,500 years (Table 4).

Although the statistical significanc the *a* peaks can hardly be in doubt, peaks *b* and *c* a more detailed exami tion and statistical evaluation are cle desirable. These objectives are achie by expressing the variance on a log sc (Fig. 6, top) and by prewhitening signal to reduce distortions in the higl frequency part of the spectrum cau by variance transfer from the *a* p during analysis. The resulting spec which have the flat trend desired (Fig bottom), should be used in the higl frequency part of the spectrum, not (to conduct statistical tests but also obtain more accurate frequency (mates.

Estimates of *b* peak frequencies in prewhitened signals are changed little; their dominant cycles now ra from 42,000 to 43,000 years (Table The *c* peaks differ mainly in the app ance of a small subsidiary peak in th spectrum. The midpoints of the thre peaks now correspond to cycles 24 years long; and the midpoints of th peaks in the *Ts* and $\delta^{18}O$ spectra cc spond to a 19,500-year cycle (Fig. 6 Table 4).

Statistical evaluation. Based on

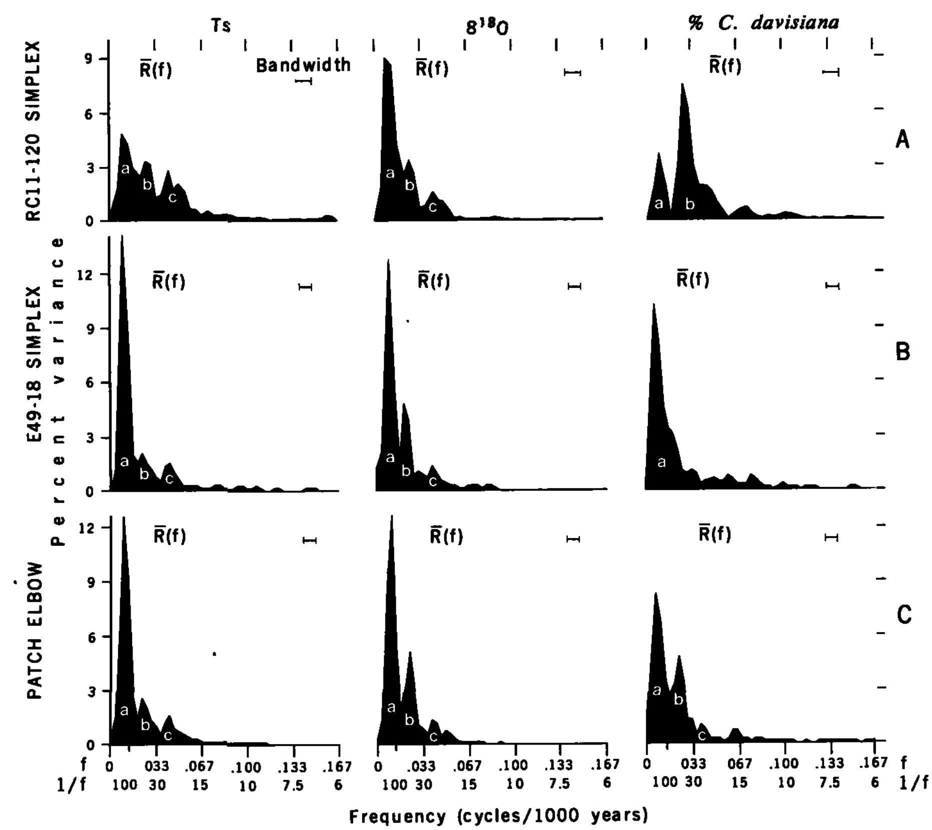

Fig. 5. High-resolution spectra of climatic variations in *Ts*, $\delta^{18}O$, and percentage of *C. davisiana*. Variance (as percentage of total variance per unit frequency band) is plotted as a function of frequency (cycles per thousand years). Prominent spectral peaks are labeled *a*, *b*, and *c*. Arrows indicate weighted mean cycle lengths (in thousands of years). The age models used in the calculations are given in Table 2. (A) Spectra for core RC11-120 are calculated for the SIMPLEX age model. (B) Spectra for core E49-18 are calculated for the SIMPLEX age model. (C) Spectra of the combined (PATCH) record are calculated for the ELBOW age model.

null hypothesis that the data are a sample of a random signal having a general distribution of variance like that in the observed low-resolution spectrum, confidence intervals are calculated as a guide to the statistical significance of spectral estimates in the high-resolution spectrum (Fig. 6). A particular peak in that spectrum is judged significant if it extends above the low-resolution spectrum by an amount that exceeds the appropriate one-sided confidence interval. Of the three *b* peaks, one is significant at $P = .02$ (*C. davisiana*) and one at $P = .05$ ($\delta^{18}O$). Of the three c_1 peaks, one (*Ts*) is significant at $P = .05$ (*65*).

We carefully considered aliasing and harmonic problems (*66*) and conclude that our spectral peaks are not an artifact of procedure. This conclusion was supported by examining more detailed spectra calculated by the maximum entropy technique (*67*).

Discussion. Having examined the confidence intervals for individual climatic spectra, and having eliminated the aliasing and harmonic problems, we can now ask if the frequencies found in the three spectra are those predicted by our linear version of orbital theory. In making this frequency-domain test we must note that the geologic spectra contain substantial variance components at many frequencies in the range of interest, and not simply ask whether there are statistically significant frequencies which match those predicted but whether the spectra observed show sufficient emphasis at the frequencies predicted to be accepted as nonrandom results (*65*). Our answer is "yes" for the following reasons: (i) Using a chronology that is completely independent of the astronomical theory, we find that modal frequencies observed in the geological record match the obliquity and precession frequencies to within 5 percent. The coherence of these results across different variables measured in two cores we regard as very powerful support for the theory. (ii) Two geological spectra ($\delta^{18}O$ and percentage of *C. davisiana*) have peaks corresponding to the predicted obliquity frequency that are significant at $P = .05$. One geological spectrum (*Ts*) has a peak corresponding to the dominant precession frequency which is also significant at $P = .05$. (iii) In addition, the predicted ratios of obliquity to precession frequencies (calculated for the time intervals represented by cores RC11-120 and E49-18) match the ratios of measured climatic frequencies in the two cores (using the SIMPLEX chronology) to within 5 percent—a result that is independent of absolute age specifications and depends only on the assumption of constant accumulation rates.

Having found the frequencies of obliquity and precession in our geological records—as predicted by a linear version of the theory of orbital control—we should consider again the lower-frequency climatic components which, although not predicted, actually contain about half of the observed variance. These components form the *a* peaks in our spectra. Concentrated at periods near 100,000 years (Figs. 5 and 6), they are close to the 105,000-year period in the eccentricity spectrum (Table 4). This similarity of the dominant frequencies in late Quaternary records of climate and eccentricity has been noted before (*13, 17, 18*) and demands an explanation. One hypothesis (developed further below) is that the radiation-climate system responds nonlinearly (*68*) to changes in the geographic and seasonal distribution of insolation. Another is that the small control eccentricity exerts on the total annual insolation is significant climatically (*59*).

An apparently independent confirmation of our conclusions about spectral peaks *b* and *c* can be found in reports of climatic periodicities in the $\delta^{18}O$ record closely matching those of obliquity and precession (*14, 16, 20, 26, 69*). However, the time scale used in these investigations differs from ours by about a factor of 2. The explanation of this paradox is to be found in the dominant climatic periodicity, which in all of the cores is the 100,000-year cycle, and not, as expected (*2, 26*), the geologic response to the 41,000-year obliquity cycle (Table 5). The spectral peak identified by Kemp and Eger (*16*) and by Chappell (*20*) as due to precession, corresponds to our *b* peak, and therefore (we argue) is actually an effect of obliquity. The spectral peak identified by van den Huevel (*14*) as due to the precession half-cycle corresponds to our *c* peak, and therefore is now to be understood as the effect of a full precession cycle. Only with the advent of chronologies based on the Brunhes-Matuyama magnetic reversal (*17, 18, 31*) was the dominant climatic period in the $\delta^{18}O$ record identified as approximately 100,000 years (Table 5).

Time-Domain Tests

Assumptions. As with the frequency-domain test, we start here with the assumption that the radiation-climate system is time-invariant and linear. One well-known characteristic of such a system forms the basis for our time-domain tests: any frequency component of the

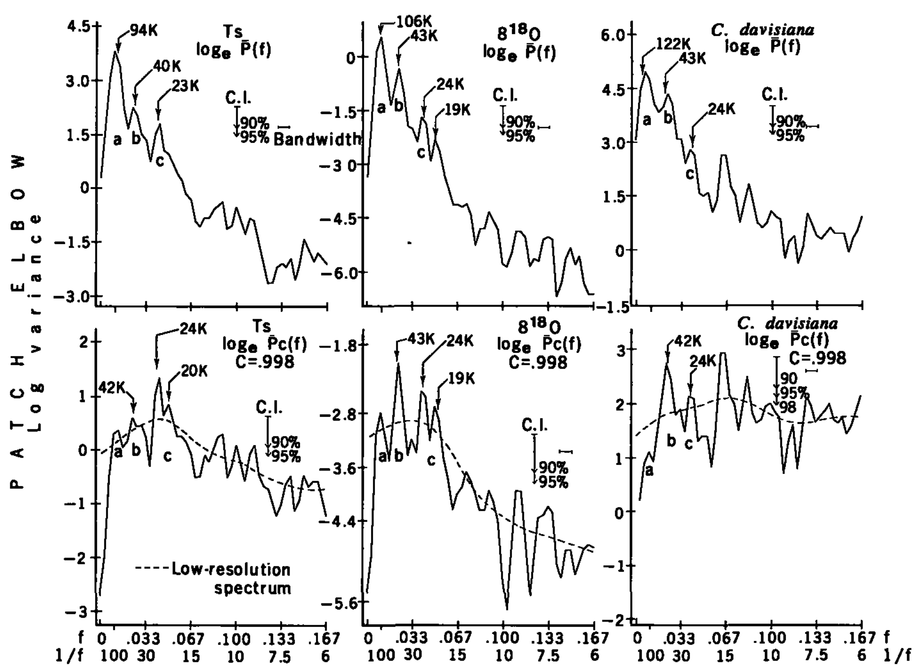

Fig. 6. Spectra of climatic variations (in *Ts*, $\delta^{18}O$, and percentage of *C. davisiana*) in the combined (PATCH) record from two subantarctic deep-sea cores. Calculations are based on the ELBOW age model (Table 2). Arrows without crossbars indicate weighted mean cycle lengths of spectral peaks (in thousands of years). Arrows with crossbars show one-sided confidence intervals (*C.I.*) attached to estimates in the high-resolution spectrum. Prominent spectral peaks are labeled *a*, *b*, and *c*. (Top row) High-resolution spectra from Fig. 5C expressed as the natural log of the variance as a function of frequency (cycles per thousand years). (Bottom row) High-resolution spectra (solid line) and low-resolution spectra (dashed line) after prewhitening with a first-difference filter.

input signal will appear at the same frequency as a component of the output, but exhibit there a certain phase shift. How much that phase shift will be we cannot say, for at any particular frequency the magnitude of the phase lag will depend not only on the time constant of the system, but also on the exact form of the system's linear response. If, for example, the system has a single-exponential response without delay, then the output will lag behind the input by no more than a quarter of a cycle. But if the system does exhibit delay, then the lag can exceed a quarter-cycle. An additional source of uncertainty attaches to the 23,000-year (but not the 40,000-year) component of the orbital input, for the phase of the precession index itself is arbitrarily defined with respect to a particular time of the year.

Although our predictive model is nonspecific, in the sense that it does not say what the shape of a particular climatic record should be, it does predict that whatever orbital-geological phase shift is observed at a particular (obliquity or precession) frequency, that shift should be constant (*19*).

Furthermore, we can assume that each climatic index reflects a response of one physical part of the climate system and is characterized by a certain time constant. Therefore, whatever phase shift is observed (at a particular frequency) between a pair of climatic indices should also be constant, and the subsystem with the larger time constant should lag the other. Because the $\delta^{18}O$ curve reflects changes in the cryosphere (a part of the climate system that must have longer time constants than the ocean), we expect that curve to lag *Ts* and percentage of *C. davisiana* at all frequencies.

Numerical procedures. Discrete spectral peaks in our geological time serie[s] have already been observed and identi[-] fied as variance components related t[o] obliquity and precession. Using a band pass digital filter (Tukey filter), we wi[ll] now extract these components from th[e] signal and display them in the time d[o]main (*70*). To use this phase-free filt[er] the investigator chooses f_0, the cent[er] frequency in the band to be studied, a[nd] fixes the bandwidth by determining r, t[he] resolution of the filter (*71*). The impact [of] a particular filter on the frequency d[o]main is described by its frequency-[re]sponse function, $H(f)$. We used two [fil]ters, one centered at a frequency of 0. cycle per 1000 years and one at 0.(cycle per 1000 years (Fig. 7). These v[will] be referred to as the 40K (40,000-ye[ar]) and 23K (23,000-year) filters, respecti[ve]ly. Their bandwidths have been cho[sen] so that the adjacent half-power poi[nts] nearly coincide, and the variance in [the] filtered signal is approximately the s[ame] as the variance in the correspon[ding] spectral peak.

Because filters of this type y[ield] smooth curves no matter what data [are] processed (*72*), the objective in u[sing] them is simply to determine in the [time] domain, and for each frequency c[om]ponent of interest, the position o[f in]flection points in the filtered record[. Al]though the average interval betwee[n in]flection points must match [the] frequency within the passband of th[e fil]ter, information in the data control[s the] exact timing of each inflection. I[Phase] shifts can be estimated visually by [com]paring two geological variables filte[red at] the same frequency, or by compari[ng an] orbital curve with a geological cur[ve fil]tered at the same frequency. Cross[-spec]tral techniques are employed on [fil]tered data to obtain for the freque[ncy of] interest a quantitative estimate of t[he av]erage phase shift over the study in[terval] (*73*).

Patterns in the geologic record[. Two] sets of curves (Fig. 8, A and C) sh[ow the] results of applying filters to the EI time series. The three geological filtered at 40K are approximat[ely in] phase throughout their length. spectral analysis shows $\delta^{18}O$ lag[ging] by 2000 years and percentage of *C* [*davis*]*iana* by 1000 years. The data filt[ered at] 23K show a nearly constant pha[se rela]tionship between $\delta^{18}O$ and percer[ntage of] *C. davisiana* throughout the reco[rd] $\delta^{18}O$ lagging percentage of *C. da*[*visiana*] by an average of 4000 years 350,000 years ago $\delta^{18}O$ system

Table 5. Comparison of published $\delta^{18}O$ chronologies and spectra. Dominant periods (in thousands of years) as calculated by investigators cited are correlated with spectral peaks *a*, *b*, and *c* documented in this article.

Chronological models		Correlation of dominant periods identified		
Age of 12-11 boundary (× 10³ years)	Reference	*a*	*b*	*c*
220*	Emiliani (*26*)	40		
220	van den Heuvel (*14*)†	40		13
240‡	Kemp and Eger (*16*)	~ 52	~ 27	
270§	Emiliani (*27*)	50		
270	Chappell (*20*)‖	~ 46	~ 25	
350	Imbrie and Kipp (*18*)¶	80	30	
375	Broecker and van Donk (*17*)	90		
380	Pisias (*82*)#			23
	This article:			
425	TUNE-UP age	99	42	22
440	ELBOW age	106	43	22

*Age calculated on the assumption that $\delta^{18}O$ stages reflect obliquity. †Data from Emiliani (*68*). ‡Age selected to match spectral peaks calculated from Emiliani's (*27*) $\delta^{18}O$ data with orbital frequencies. §Age calculated by extrapolation beyond a section of the curve estimated to be younger than 150,000 years by early results of the Pa/Th technique. ‖Data from Emiliani (*27*). ¶Data for $\delta^{18}O$ from Broecker and van Donk (*17*); an unconformity was later recognized in this record (*78*). #Data for $\delta^{18}O$ from Shackleton and Opdyke (*31*).

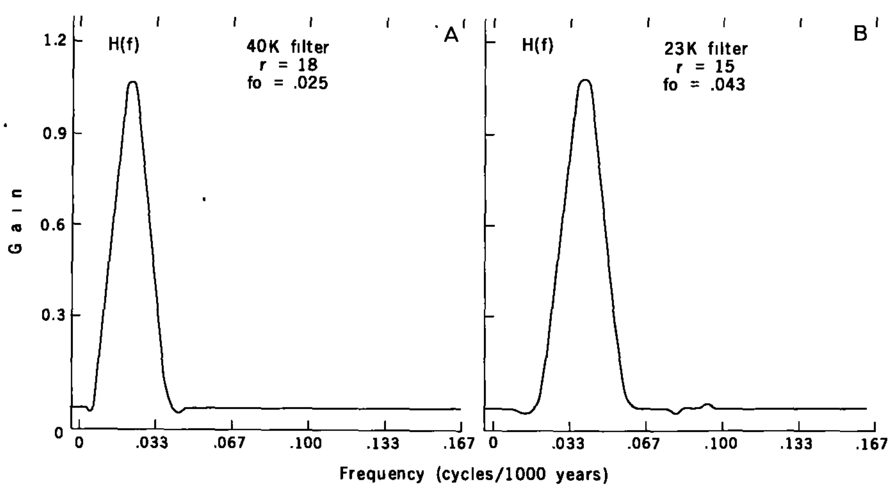

Fig. 7. Gain function for band-pass filters used to calculate curves in Figs. 8 and 9: (A) 40K filter centered on a frequency of 0.025 cycle per thousand years; (B) 23K filter centered on a frequency of 0.043 cycle per thousand years. Tukey filters were used (*70*).

Ts by an average of about 2000 ;. Before that time, however, $\delta^{18}O$ *Ts* are clearly out of phase.

ıe general pattern of these relation- ; can be observed on the strati- hic diagrams (Figs. 2 and 3) and is in- ·ndent of assumptions about chronol- Therefore, the climate changes of wo hemispheres are nearly in phase ng the last 300,000 years with ıges in the Southern Hemisphere ın appearing to lead changes in the thern Hemisphere ice sheets by up to w thousand years. However, before 000 years ago *Ts* and $\delta^{18}O$ appear to ›ut of phase in the 23K but not the . frequency band.

rbital-geologic phase relationships. played on the ELBOW chronology, se relationships between the filtered lögical curves and orbital curves are tematic over the past 300,000 years ;. 8, A and C); that is, back to the up- part of stage 9. Over that interval, es of low temperature, high $\delta^{18}O$ ra- ;, and abundant *C. davisiana* follow .es of low obliquity. The 40K com- ıents of the geological curves (Fig.) lag obliquity by about a quarter- :le. Measurements made at the maxi- ι and minima of 12 obliquity half-cy- :s covering the interval 70,000 to),000 years ago show that $\delta^{18}O$, *Ts*, d percentage of *C. davisiana* lag obliq- .y by 9000 ± 3000, 8000 ± 3000, and 00 ± 4000 years, respectively. Below e top of stage 9, however, the geologi- .l curves on the average lead obliquity ' several thousand years.

Over the interval 0 to 150,000 years ;o on the ELBOW time scale, the inter- ıl that has the most certain chronology, ıe 23,000-year components of the geo- ıgical curves systematically lag pre- ɜssion by about 3000 years (Fig. 8A). lowever, when averaged over the inter- al 0 to 300,000 years they are approxi- ıately in phase with precession. Mea- ɹrements made at the maxima and mini- ıa of 22 precession half-cycles covering he interval 50,000 to 300,000 years ago how that $\delta^{18}O$, *Ts*, and percentage ›f *C. davisiana* lag precession by .500 ± 3500, 0 ± 3000, and –500 ± 4500 /ears, respectively. Times of low temper- ıture, high $\delta^{18}O$ ratios, and abundant *C. lavisiana* are associated with times of high positive values of the precession in- dex—that is, times when the earth-sun distance in June is greater than normal. The systematic orbital-geologic phase relationships just described do not, how- ever, exist below the 300,000-year hori- zon. There, a confusing pattern of leads and lags among all of the curves is dis- played.

Discussion. We regard the results of the time-domain test as strong evidence of orbital control of major Pleistocene climatic changes, for the following reasons: (i) Over the past 300,000 years, each of the 40K components of the geological records exhibits a phase relationship with obliquity which is as constant as could be expected from a geological record. Monte Carlo tests we have conducted with our filters show that the degree of regularity observed would be highly unlikely as a random result. The magnitude of the phase shift (7000 to 9000 years) is less than a quarter of the cycle length. (ii) Averaged over the same interval, the 23K components of the geological curves exhibit in-phase relationships with precession which are as constant as could be expected from a geological record. Again, the observed regularity is too great to be explained as a random result. When the chronology is most accurate for the filtered record (50,000 to 150,000 years ago), the 23K components of the geological curves lag

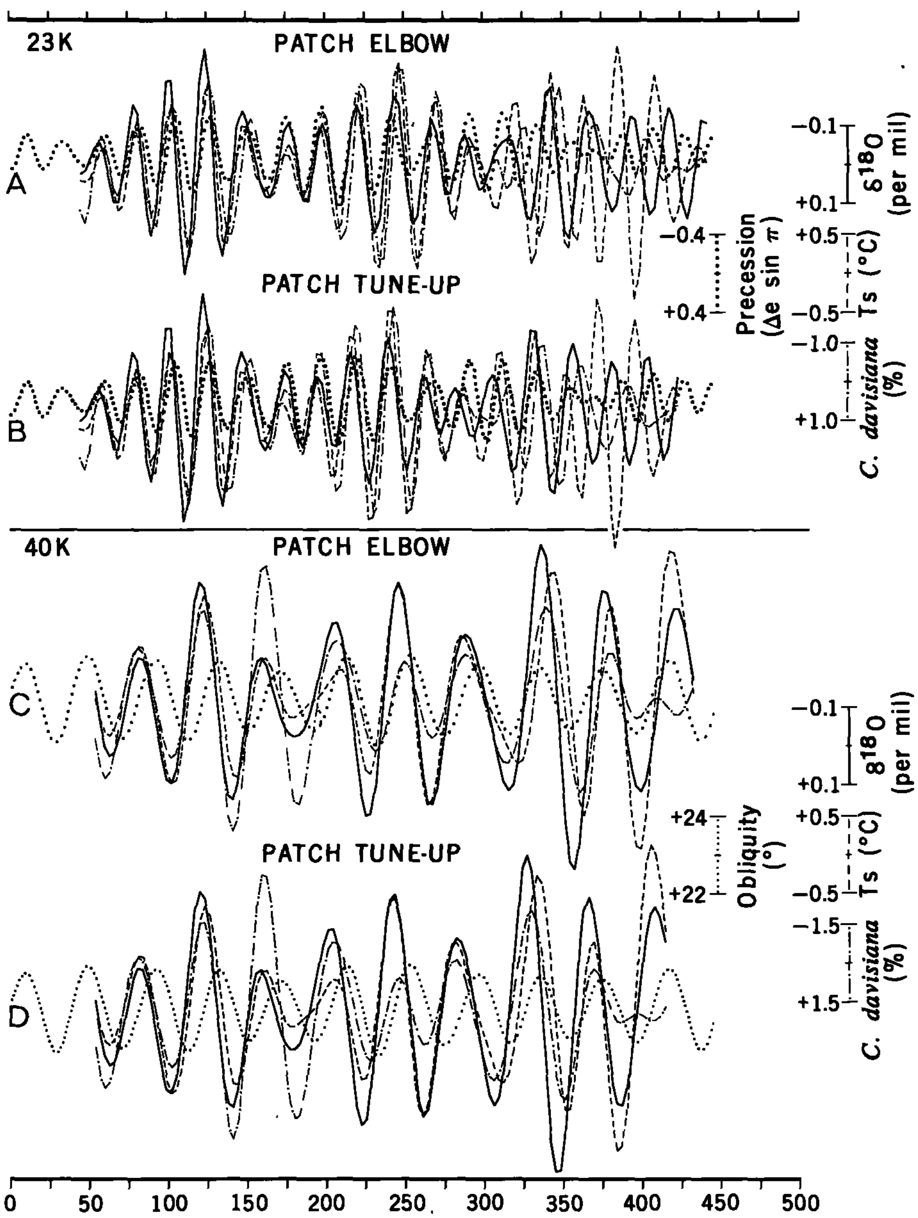

Fig. 8. Variations in obliquity, precession, and the corresponding frequency components of climate over the past 500,000 years. Orbital data are from Vernekar (*39*). Climatic curves are variations in $\delta^{18}O$, *Ts*, and percentage of *C. davisiana* plotted against alternate geological time scales (ELBOW and TUNE-UP) as defined in Table 2. The variations shown are frequency components extracted from the raw-data curves by means of digital band-pass filters (Fig. 7). The two sets of curves in (A) and (B) include the precession curve and the 23,000-year frequency components of climate based on the ELBOW (A) and TUNE-UP (B) time scales. The two sets of curves in (C) and (D) include the obliquity curve and the 40,000-year frequency components of climate based on the ELBOW (C) and TUNE-UP (D) time scales.

precession by about 3000 years. (iii) The expectation that the 23K and 40K components of the $\delta^{18}O$ curve should show a constant lag against the corresponding components of *Ts* and percentage of *C. davisiana* is confirmed by the geological record of the last 350,000 years. The out-of-phase relationship between *Ts* and $\delta^{18}O$ that appears in stage 10 and the upper part of stage 11 may be related to the low amplitudes of precession variation resulting from near-zero eccentricity at this time. This may have allowed a decoupling of *Ts* variation from precession over this short interval. (iv) The fact that the large irregularities which do occur in the observed orbital-geologic phase relationships at both frequencies are stratigraphically concentrated in the early part of the record (before 300,000 years ago) where the chronology is least accurate, rather than randomly distributed, suggests that these irregularities result from errors in the older chronology.

Implications of Test Results

Quaternary time scale. Taken together with the results of the frequency-domain test, the systematic phase relationships just described suggest that a small error occurs in the older portions of the ELBOW chronology. To explore this hypothesis we have made the minimum adjustments in the ELBOW chronology which would extend farther back in time the systematic phase relationships observed in the younger parts of the ELBOW record. These adjustments (Table 2) are easily within the absolute error of the radiometric dates on which the ELBOW time scale is based. On this revised chronology (called TUNE-UP), the age of the isotope stage 11-12 boundary is reduced by 3 percent (25,000 years), and the age of isotope stage 7-8 boundary is reduced by 2 percent (4000 years) (Table 6).

The impact of these adjustments in the time domain (Fig. 8, B and D) is to extend the systematic phase relationships previously noted with obliquity back over the whole range of the filtered record—some 425,000 years. There is also a definite improvement in the phase relationship with precession. For the $\delta^{18}C$ record, this relationship is generally regular and includes 13 cycles extending bacl 340,000 years. For *Ts* the relationship extends back 325,000 years, and for the percentage of *C. davisiana* back 280,00 years (with one exception near 240,00 years). We have experimented with otl er ages for our chronological contr points and find that further adjustmen result in a deterioration of the match b tween orbital parameters and the geolog cal records filtered at the same fr quencies (*74*). In the frequency domai estimates for spectral peaks calculat from the TUNE-UP time series mat those predicted for obliquity and p cession within 1000 years (Table 5).

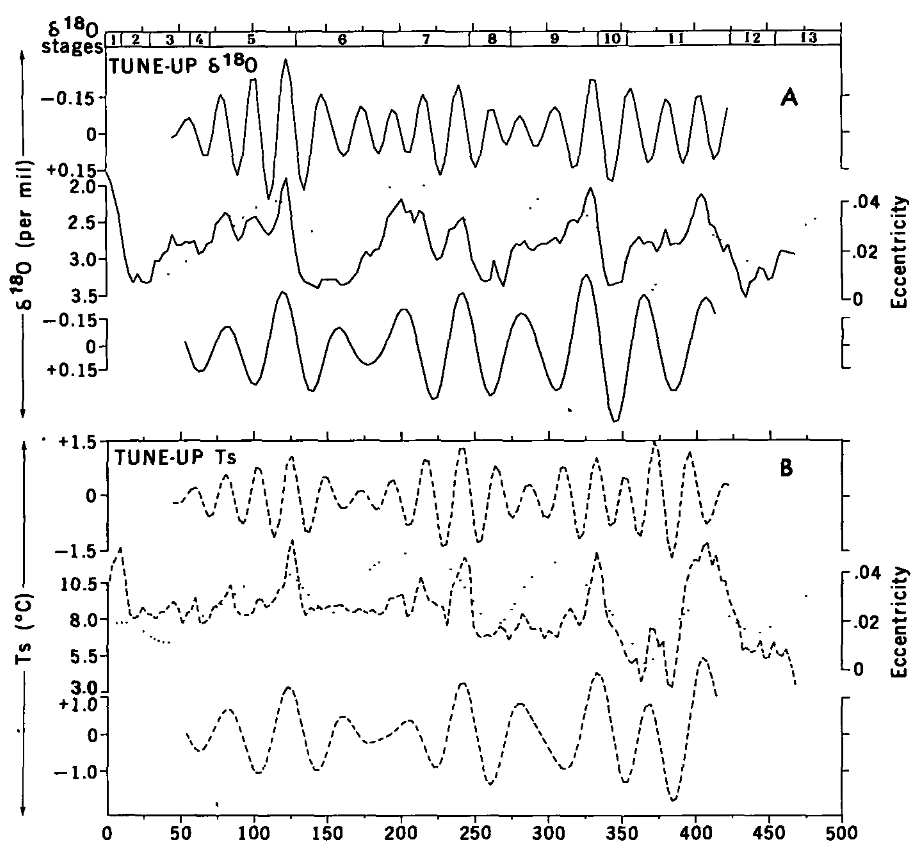

Fig. 9. Variations in eccentricity and climate over the past 500,000 years. Climatic curves are obtained from the combined (PATCH) record of two subantarctic deep-sea cores and plotted on the TUNE-UP time scale (Table 2). (A) Solid line in center shows variations in $\delta^{18}O$. Dotted line is a plot of orbital eccentricity (*39*). Upper curve is the 23,000-year frequency component extracted from $\delta^{18}O$ by a band-pass digital filter (Fig. 6). Lower curve is the 40,000-year frequency component extracted from $\delta^{18}O$ by a band-pass digital filter (Fig. 6). (B) Dashed line in center shows variations in estimated sea-surface temperature (*Ts*). Dotted line is a plot of orbital eccentricity data from Vernekar (*39*). Upper curve is the 23,000-year frequency component extracted from *Ts* by a band-pass digital filter (Fig. 6). Lower curve is the 40,000-year frequency component extracted from *Ts* by a band-pass digital filter (Fig. 6).

The 100,000-year cycle. The domina cycles in all of our spectra (Fig. 5C a Table 4) are about 100,000 years long an observation which merely confirm geological opinion now widespread (*18, 75–77*). Yet this cycle would not ar as a linear response of the climate s tem to variations in obliquity and p cession. Mesolella *et al.* (*15*) and Broe er and van Donk (*17*) account for cycle by relating it to eccentricity o the phasing of obliquity with precess Our data, displayed on a time scale rived without reference to eccentric dramatically confirm the empirical a ciation of glacial times with interval low eccentricity (Fig. 9).

Because this time-domain m agrees with independent evidence ir frequency domain ($\delta^{18}O$ and *Ts* in T 4), we conclude, as others have (*15*, that the 100,000-year climate-cyc driven in some way by changes in or eccentricity. As before, we avoid th ligation of identifying the physical n anism of this response, and instead acterize the behavior of the system in general terms. Specifically, we don the assumption of linearity (*7* such a nonlinear system (*68*) ther many ways in which the modulati fect of eccentricity on the precessi dex could generate 100,000-year ance components in the geologica ord. Among these we are attracte hypothesis that ice sheets waste than they grow; that is, that two dil time constants of the cryosphere sponse to orbital forcing are inv This concept (*79*) can be deduced logically (*7*) or arrived at indu the climatic record (*17*). Because mplitude of each precession-index is proportional to eccentricity, a nonlinear response of the ice :s would bring out the 100,000-year ıtricity signal in the geologic record ɔrcing the mean of the 23,000-year ıtic cycle to approach values directoportional to eccentricity.

ture climate. Having presented evie that major changes in past climate : associated with variations in the getry of the earth's orbit, we should be to predict the trend of future cli-:. Such forecasts must be qualified in ways. First, they apply only to the ral component of future climatic ds—and not to such anthropogenic :ts as those due to the burning of fosɹels. Second, they describe only the ;-term trends, because they are ed to orbital variations with periods 0,000 years and longer. Climatic ositions at higher frequencies are not licted.

ne approach to forecasting the natu-.ong-term climate trend is to estimate time constants of response necessary ɜxplain the observed phase relationɔs between orbital variation and cliic change, and then to use those time ıstants in an exponential-response del. When such a model is applied to rnekar's (*39*) astronomical projec-ɪs, the results indicate that the longm trend over the next 20,000 years is vard extensive Northern Hemisphere .ciation and cooler climate (*80*).

mmary

1) Three indices of global climate have èn monitored in the record of the past 0,000 years in Southern Hemisphere :ean-floor sediments.

2) Over the frequency range 10^{-4} to $^{-5}$ cycle per year, climatic variance of ese records is concentrated in three disete spectral peaks at periods of 23,000, !,000, and approximately 100,000 ɜars. These peaks correspond to the ɔminant periods of the earth's solar orit, and contain respectively about 10, 5, and 50 percent of the climatic varince.

3) The 42,000-year climatic component as the same period as variations in the bliquity of the earth's axis and retains a onstant phase relationship with it.

4) The 23,000-year portion of the vari-.nce displays the same periods (about :3,000 and 19,000 years) as the quasi-peiodic precession index.

5) The dominant, 100,000-year climatic component has an average period close to, and is in phase with, orbital eccentricity. Unlike the correlations between climate and the higher-frequency orbital variations (which can be explained on the assumption that the climate system responds linearly to orbital forcing), an explanation of the correlation between climate and eccentricity probably requires an assumption of nonlinearity.

6) It is concluded that changes in the earth's orbital geometry are the fundamental cause of the succession of Quaternary ice ages.

7) A model of future climate based on the observed orbital-climate relationships, but ignoring anthropogenic effects, predicts that the long-term trend over the next several thousand years is toward extensive Northern Hemisphere glaciation.

Table 6. Estimates of the ages of stage boundaries based on the TUNE-UP chronology. Except for the lowest two boundaries, the estimates are considered accurate within a range of +5000 to −1000 years (*74*).

Isotopic stage boundary	Depth in core (cm)		Age (× 10^3 years)
	RC11-120	E49-18	
2-1	40		10
3-2	105		29
4-3	215		61
5-4	255		73
6-5	440	490	127
7-6	620	640	190
8-7	785	825	247
9-8	900	920	276
10-9		1115	336
11-10		1180	356
12-11		1405	~ 425
13-12		1510	~ 457

References and Notes

1. R. F. Flint, *Glacial and Quaternary Geology* (Wiley, New York, 1971); J. M. Mitchell, Jr., in *The Quaternary of the United States*, H. E. Wright, Jr., and D. G. Frey, Eds. (Princeton Univ. Press, Princeton, N.J., 1965), pp. 881–901.
2. C. Emiliani and J. Geiss, *Geol. Rundsch.* **46**, 576 (1957).
3. B. Dennison and V. N. Mansfield, *Nature (London)* **261**, 32 (1976); F. Hoyle and R. A. Lyttleton, *Proc. Cambridge Philos. Soc.* **35**, 405 (1939).
4. M. Milankovitch, *K. Serb. Akad. Beogr. Spec. Publ. 132* (1941) (translated by the Israel Program for Scientific Translations, Jerusalem, 1969).
5. J. P. Kennett and R. C. Thunell, *Science* **187**, 497 (1975).
6. G. Wollin, D. B. Ericson, W. B. F. Ryan, J. H. Foster, *Earth Planet. Sci. Lett.* **12**, 175 (1971); G. Wollin, D. B. Ericson, W. B. F. Ryan, *Nature (London)* **232**, 549 (1971).
7. J. Weertman, *J. Glaciol.* **5**, 145 (1964).
8. A. T. Wilson, *Nature (London)* **201**, 147 (1964).
9. M. Ewing and W. L. Donn, in *Polar Wandering and Continental Drift* (Society of Economic Paleontologists and Mineralogists, Tulsa, Okla., 1956), pp. 94–99.
10. G. N. Plass, *Tellus* **8**, 140 (1956).
11. R. E. Newell, *Quat. Res. (N.Y.)* **4**, 117 (1974).
12. E. N. Lorenz, *Meteorol. Monogr.* **8**, 1 (1968).
13. W. S. Broecker, *Science* **151**, 299 (1966); ______, D. L. Thurber, J. Goddard, T.-L. Ku, R. K. Matthews, K. J. Mesolella, *ibid.* **159**, 297 (1968).
14. E. P. J. van den Heuvel, *Geophys. J. R. Astron. Soc.* **11**, 323 (1966).
15. K. J. Mesolella, R. K. Matthews, W. S. Broecker, D. L. Thurber, *J. Geol.* **77**, 250 (1969).
16. W. C. Kemp and D. T. Eger, *J. Geophys. Res.* **72**, 739 (1967).
17. W. S. Broecker and J. van Donk, *Rev. Geophys. Space Phys.* **8**, 169 (1970).
18. J. Imbrie and N. G. Kipp, in *The Late Cenozoic Glacial Ages*, K. K. Turekian, Ed. (Yale Univ. Press, New Haven, Conn., 1971), pp. 71–182.
19. G. Kukla, *Boreas* **1**, 63 (1972); *Nature (London)* **253**, 600 (1975).
20. J. Chappell, *Quat. Res. (N.Y.)* **3**, 221 (1973).
21. W. Koppen and A. Wegener, *Die Klimate der Geologischen Vorzeit* (Berlin, 1924).
22. N. J. Shackleton, *The Phanerozoic Time-Scale* (Geological Society, London, 1971), part 1, pp. 35–38.
23. A. Bloom, W. S. Broecker, J. Chappell, R. K. Matthews, K. J. Mesolella, *Quat. Res. (N.Y.)* **4**, 185 (1974).
24. T.-L. Ku, M. N. Kimmel, W. H. Easton, and T. J. O'Neil [*Science* **183**, 959 (1974)] document only the oldest of the terraces.
25. M. L. Bender, F. T. Taylor, R. K. Matthews, *Quat. Res. (N.Y.)* **3**, 142 (1973).
26. C. Emiliani, *J. Geol.* **63**, 538 (1955).
27. ______, *ibid.* **74**, 109 (1966).
28. More than a century ago, J. Croll [*Climate and Time* (Appleton, New York, 1875)] of Scotland employed the same basic strategy. He compared astronomical calculations of orbital history with the geologic record of climate, and pointed to evidence of multiple glaciations as confirming the astronomical theory of the ice ages.
29. W. L. Donn and D. M. Shaw, *Science* **157**, 722 (1966); J. M. Suarez and I. M. Held, in *Proceedings of the WMO/IAMAP Symposium on Long Term Climatic Fluctuations* (World Meteorological Organization, Geneva, Switzerland, 1975).
30. The raw data on which this study is based will be published (J. D. Hays, A. D. Vernekar, J. Imbrie, N. J. Shackleton, in preparation).
31. N. J. Shackleton and N. D. Opdyke, *Quat. Res. (N.Y.)* **3**, 39 (1973).
32. N. J. Shackleton, *Colloq. Int. CNRS* **219**, 203 (1974).
33. ______, *Nature (London)* **215**, 15 (1967); W. Dansgaard and H. Tauber, *Science* **166**, 449 (1969).
34. J. Lozano and J. D. Hays, *Geol. Soc. Am. Mem.* **145** (1976), pp. 303–336.
35. J. D. Hays, J. Lozano, N. Shackleton, G. Irving, *ibid.*, pp. 337–372.
36. M. G. Petrushevskaya, in *Biological Reports of the Soviet Antarctic Expedition (1955–1958)*, A. P. Andriyashev and P. V. Ushakov, Eds. (Leningradskoe Otdelenie, Leningrad, 1967; Israel Program for Scientific Translations, Jerusalem, 1968), p. 2.
37. J. H. Robertson, thesis, Columbia University (1975).
38. A. J. van Woerkom, *Climatic Change* (Harvard Univ. Press, Cambridge, Mass., 1953), pp. 147–157; S. G. Sharaf and N. A. Budnikova, *Tr. Inst. Teor. Astron.* **11**, 231 (1967) (translated by the Clearinghouse for Federal Scientific and Technical Information, Springfield, Va.).
39. A. D. Vernekar, *Meteorol. Monogr.* **12** (1972).
40. A. L. Berger, *Astron. Astrophys.*, in press.
41. N. J. Shackleton and N. D. Opdyke, *Geol. Soc. Am. Mem.* **145** (1976), pp. 449–464; CLIMAP Project Members, *Science* **191**, 1131 (1976).
42. D. Ninkovich and N. J. Shackleton, *Earth Planet. Sci. Lett.* **27**, 20 (1975).
43. H. Thierstein, K. Geitzenauer, B. Molfino, N. J. Shackleton, in preparation; S. Gartner, *Palaeogeogr. Palaeoclimatol. Palaeoecol.* **12**, 169 (1972).
44. J. D. Hays and N. J. Shackleton, in preparation.
45. T. Kellogg, in *Climate of the Arctic*, G. Weller and S. A. Bolliny, Eds. (Geophysical Institute, Univ. of Alaska, Fairbanks, 1975), pp. 3–36; *Geol. Soc. Am. Mem.* **145** (1976), pp. 77–110.
46. J. D. Hays and D. Ninkovich, *Geol. Soc. Am. Mem.* **126** (1970), p. 263; J. D. Hays and N. Opdyke, *Science* **158**, 1001 (1967).
47. We have used only those ages for the stage 12-11 boundary based on interpolations between the core top and the Brunhes-Matuyama magnetic reversal. Although Hays *et al.* [J. D. Hays, T. Saito, N. D. Opdyke, L. H. Burckle, *Geol. Soc. Am. Bull.* **80**, 1481 (1969)] estimated the time of extinction of *Stylatractus universus* by this method and obtained an estimate of 341,000

years, Shackleton and Opdyke (*31*) argued convincingly that this estimate was too young, because of sedimentation rate changes between the lower and upper Brunhes magnetic series. We have not used estimates based on Io/Th techniques because we believe the intrinsic inaccuracy of these estimates is large.
48. C. Emiliani and N. J. Shackleton, *Science* **183**, 511 (1974).
49. E. Rona and C. Emiliani, *ibid.* **163**, 66 (1969).
50. H. H. Veeh and J. M. A. Chappell, *ibid.* **167**, 862 (1970).
51. T.-L. Ku and W. S. Broecker, *ibid.* **151**, 448 (1966).
52. C. Sancetta, J. Imbrie, N. G. Kipp, *Quat. Res. (N.Y.)* **3**, 110 (1973).
53. L. A. Zadeh and C. A. Desoer, *Linear System Theory* (McGraw-Hill, New York, 1963), p. 628.
54. In this section of the article we have benefited from discussions with W. A. Wolovich.
55. G. M. Jenkins and D. G. Watts, *Spectral Analysis and Its Applications* (Holden-Day, San Francisco, 1968).
56. R. B. Blackman and J. W. Tukey, *The Measurement of Power Spectra from the Point of View of Communication Engineering* (Dover, New York, 1958), p. 190.
57. The procedures are as follows: (i) Selection of an absolute chronology. For astronomical variables, we adopt the chronology of Vernekar (*39*). For geological variables, we use our chronological models discussed above. (ii) Calculation of a time series. A uniform sampling interval (Δt) approximately equal to the average interval between sample points is chosen (in this study, 3000 years), and a time series of n values is calculated by linear interpolation. For the PATCH time series, n ranges from 157 to 163 according to the chronology used. (iii) Detrending. Any long-term trend is removed by calculating residuals from linear regression. (iv) Prewhitening. If the spectrum is dominated by low-frequency components the signal may be prewhitened by means of a first-difference filter in which the intensity of the prewhitening is controlled by a constant, C. In our study, $C = 0.998$ (*56*). (v) Lagging. The number of lags (m) to be used in the next step is chosen according to the bandwidth (amount of detail) desired in the estimated spectrum. (vi) Calculation of autocovariance function. The covariance between the original time series and each of m lagged versions is calculated. (vii) Smoothing. The autocovariance function, smoothed by a Hamming lag window, yields a bandwidth of approximately $1.258/m\Delta t$ cycles per thousand years. To establish the general trend of the spectrum, we fix m as 8; the resulting spectrum has high accuracy but low resolution. For more detail, m is fixed at 40 to 50, depending on n. (viii) Spectral estimation. Variance contributions to each of $m + 1$ frequency bands are calculated by a Fourier transform of the smoothed autocovariance function. The resulting spectrum has a frequency range from zero to the Nyquist frequency ($fn = 1/2\Delta t$), the highest frequency that can be determined with a given Δt. Frequencies in cycles per thousand years are plotted on a linear scale; a reciprocal scale indicates cycle length in thousands of years. (ix) Scaling. The initial estimates of an unprewhitened signal specify variance ("power") as a function of frequency, that is, $P(f)$. For prewhitened spectra, the corresponding symbol is $Pc(f)$. To simplify the use of confidence intervals, variance is expressed on a log scale. To facilitate the comparison of spectra calculated from variables with different scales, values of $P(f)$ are rescaled as $\bar{R}(f)$ so that the area under the curve equals unity. (x) Statistical evaluation. A one-sided confidence interval attached to each estimate in the high-resolution spectrum is calculated from the chi-square distribution, using $2n/m$ degrees of freedom, and expressed on a log scale (*55*, *56*). Calculations in steps iii through viii were carried out with a BMDO2T program (*58*) modified by Y. Yeracaris to avoid recoloring the spectrum when the prewhitening option is used.
58. W. J. Dixon, Ed., *BMD Biomedical Computer Programs* (Los Angeles School of Medicine, Univ. of California, Los Angeles, 1965), p. 620.
59. A. L. Berger [in *Symposium on Long-Term Climatic Fluctuations*, Norwich, August, 1975 (World Meteorological Organization, Geneva, 1975), pp. 65–72] concludes that variations in eccentricity are positively correlated with planetary insolation receipt, and that, although small, this effect might be climatically significant.
60. Changes in Π reflect the interaction of precession with the changing orientation of the orbital ellipse.
61. This interpretation of the precession curve, due to Broecker and van Donk (*17*), was confirmed by A. L. Berger (personal communication) as accurate to the first order of the earth's eccentricity.
62. Digital data were provided by A. D. Vernekar.
63. We have estimated astronomical frequencies by two methods: averaging the number of peaks in the time domain, and spectral analysis (Tables 3 and 4). The averaging gives satisfactory results for simple sinusoidal curves such as obliquity, but cannot resolve the component frequencies in more complex precession, insolation, or climate curves. For uniformity, spectral estimates are used exclusively in this article.
64. Higher-resolution spectra of much longer eccentricity records actually have two discrete peaks (corresponding to periods of 96,000 and 125,000 years).
65. Discussions with J. W. Tukey were helpful in framing statistical hypotheses and in properly prewhitening the signals.
66. Questions of sampling variance apart, there are two ways in which our results might be artifacts of procedure. First, the *b* and *c* peaks could be aliases of cycles present in the cores but not visible in our data because their frequencies are higher than the Nyquist frequency. However, the mixing of deep-sea sediments by bottom-living animals rules out the possibility that signals with sufficient power at these frequencies could remain in the record. Second, a significant part of the variance in the data for $\delta^{18}O$ and particularly for *Ts* has the form of a Dirac comb—that is, has equally spaced spikes (Figs. 2 and 3). As the Fourier transform of a comb yields a comblike spectrum with frequencies that are harmonics of the fundamental, it might be supposed that our *b* and *c* peaks (42,000, 24,000, and 19,500 years) could be statistically blurred versions of the third, fifth, and sixth harmonics of a fundamental 122,000-year cycle (~ 41,000, ~ 24,000, and ~ 20,000 years). But several arguments can be advanced which eliminate this possibility: (i) No discrete spectral peaks occur at frequencies corresponding to the second and fourth harmonics (61,000 and ~ 30,000 years) of the presumed fundamental. (ii) The dominant frequencies of peaks *b* and *c* are not harmonics of the dominant cycles we estimate in *a* (94,000 years for *Ts* and 106,000 years for $\delta^{18}O$). (iii) Although the percentage of *C. davisiana a* peak actually has a dominant period near 122,000 years, and its 42,000-year spectral peak is strongly developed, this time series does not approach a Dirac comb.
67. This method [R. T. Lacoss, *Geophysica* **36**, 661 (1971)] was applied to our data by T. E. Landers, Lincoln Laboratory, Massachusetts Institute of Technology.
68. H. S. Tsien, *Engineering Cybernetics* (McGraw-Hill, New York, 1952), p. 164.
69. C. Emiliani, *Ann. N.Y. Acad. Sci.* **95**, 521 (1961).
70. N. R. Goodman, *J. Franklin Inst.* **270**, 437 (1960).
71. The larger the value of r, the narrower the passband. Because the filter is an array of $2r + 1$ weights for a moving average applied in the time domain, r data points are lost at the end of] filtered signal. All of our filter calculations w carried out with a BMDO1T program (*58*).
72. E. Slutsky, *Econometria* **5**, 105 (1937).
73. Cross-spectral techniques (*55*) were first appl to deep-sea cores by Moore *et al.* [T. C. Moc Jr., N. Pisias, G. R. Heath, in *The Fate of Fo. Fuel CO_2* (Plenum, New York, in press)].
74. In arriving at the TUNE-UP chronology, first experimented with ages of the stage 12 boundary ranging from 380,000 to 440,000 ye ago, while retaining the stage 6-5 and youn ELBOW control points (Table 2). The ph coherences between the orbital and filtered g logical signals reached a maximum in these periments when the 12-11 boundary was fixe 425,000 years. With that boundary determir we then experimented with different ages of 8-7 and 6-5 boundaries to arrive at the TU UP chronology. To evaluate the uncertaint this chronology over the interval 50,00(350,000 years ago (where we can check pl coherence at both frequencies) we next ducted trials in which the three oldest TU UP control points were all shifted by the s experimental interval, while holding cons the 9400-year level dated by carbon-14 and zero-age core top. With a shift of either plu minus 22,000 years (that is, an interval equ an average precession cycle and approxim equal to half an obliquity cycle), the phase co ences are drastically disturbed in the you part of the record. A final experimental seri which the three oldest TUNE-UP control p were shifted together over a range of ± years shows that the only chronologies w serious consideration (under the hypothes phase coherence at the frequencies of obli and precession) show deviations from TUNE-UP values ranging between +500(−1000 years, with the optimum phase ma from 50,000 to 350,000 years ago being close to that fixed by the TUNE-UP chron (Table 2).
75. G. Kukla, *Geol. Foeren. Stockholm Foerh* 148 (1970).
76. W. F. Ruddiman and A. McIntyre, *Geol. Am. Mem.* **145** (1976), pp. 111–146.
77. U.S. Committee for the Global Atmos Research Program, National Research Co *Understanding Climatic Change, A Progra Action* (National Academy of Sciences, ington, D.C., 1975), figure A-14.
78. J. Imbrie, J. van Donk, N. G. Kipp, *Quat (N.Y.)* **3**, 10 (1973).
79. N. Calder, *Nature (London)* **252**, 216 (19
80. J. Imbrie and J. Z. Imbrie, in preparation
81. J. Hülsemann, *J. Sediment. Petrol.* **3** (1966).
82. N. G. Pisias, *Geol. Soc. Am. Mem.* **145** (pp. 375–392.
83. Supported by NSF IDOE grants IDO 71 and OCE 75-19627 to Lamont-Doherty G cal Observatory of Columbia University grant OCD 75-14934 to Brown Universit NERC grant GR 3/1762 to Cambridge Un ty, England. We are grateful to those whc rially contributed to this article in the fol ways: data generation, G. Irving, K. Jare larian counts), M. A. Hall (operation o Micromass mass spectrometer), A. Ve (orbital and insolation data in digital forr A. L. Berger (digital data on seaso solations); data processing, Y. Yerac Morley, N. Kipp, D. Kirkpatrick, anc Imbrie; production of manuscript, R. M. M. Perry, and R. Mellor. We are also gra all those who freely contributed their id critically read the manuscript; in partic wish to thank J. M. Mitchell, Jr., A. (Hughes, J. W. Tukey, G. Kukla, A. Ber S. Sachs. We are grateful to all our C colleagues who encouraged and critici work during the past 2 years. This a Lamont-Doherty Geological Observato tribution 2434.